Adsorption 2, 51–58 (1996)

Topologies of Capillary Condensation

M.J. BOJAN
Department of Chemistry, The Pennsylvania State University, University Park, PA 16802

E. CHENG
Department of Physics, The Pennsylvania State University, University Park, PA 16802; and Department of Chemistry, University of California, Berkeley, CA 94720

M.W. COLE
Department of Physics, The Pennsylvania State University, University Park, PA 16802

W.A. STEELE
Department of Chemistry, The Pennsylvania State University, University Park, PA 16802

Abstract. Calculations are presented to illustrate the dependence of capillary adsorption upon the interactions present in model pores. The sequence of phase transitions at zero temperature is determined for a Lennard-Jones lattice gas in a pore consisting of $4 \times 4 \times \infty$ sites. The dependence of the specific filling sequence upon the comparative strength of the gas-pore wall and the gas-gas interaction well-depths is determined. Grand canonical Monte Carlo simulations of sorption at finite temperature in the continuum version of the same model pore are also reported. Both the theory and the simulations were performed with variable gas-solid and gas-gas energy well-depths. At a temperature of 90 K, the gas-solid heterogeneity associated with atoms adsorbed in the corners, on the walls and in the interior pore volume gives rise to sequential adsorption similar to that observed in the lattice gas calculation at 0 K. A gradual approach to non-wetting behavior is observed as the gas-solid well-depth decreases. Values of the gas-solid well-depth needed to produce pore filling at saturation (i.e., "pore-wetting") are discussed.

Keywords: adsorption in pores, computer simulation, wetting, heterogeneity

1. Introduction

The venerable subject of capillary condensation continues to attract attention for both basic scientific and technological reasons (Gregg and Sing, 1982). Scientists have been particularly interested in the principles underlying the very diverse kinds of behavior observed experimentally. The reliability of theoretical predictions of this behavior is often limited because of the need for simplifying assumptions about the pore geometry and the fluid-pore wall interaction laws. Nevertheless, generic predictions are possible about trends expected in the adsorption process, as this paper exemplifies.

The question addressed here is how adsorption proceeds under varying assumptions about the relative interactions in the problem. It is obvious, for example, that adsorption is enhanced (diminished) if the adsorbate is strongly (weakly) attracted to the adsorbent. A detailed description of this dependence is one of our principal goals.

Our analysis consists of two distinct but related aspects. In Sections 3 and 4, we consider sorption in an extremely simple model pore with smooth planar walls, infinite length and a square cross-section. The size of the cross-section is chosen so that 4×4 argon atoms will be accommodated in it if a gas-wall energy is chosen that is appropriate for the argon-graphite basal

plane interaction. In Section 2, the details of the model are specified and it is further assumed that the adsorbed atoms are located on a lattice which is $4 \times 4 \times \infty$ simple cubic. In Section 3, the pore-filling properties of this model at zero temperature are evaluated as a function of the interaction well-depths, both gas-gas and gas-solid. In Section 4, the properties of these systems are evaluated with the lattice gas restriction removed. In this case, thermodynamic properties were obtained by performing grand canonical Monte Carlo simulations for a finite temperature (90 K).

In both studies, transitions in the sorption isotherms are found that are associated with sequential filling of various regions within the pore (corners, walls, interior volumes). The changes in these transitions produced by altering the strength of the gas-gas and the gas-solid interactions are characterized. One of the more interesting results is that the pore becomes "non-wet" as the gas-solid well-depth is decreased to a value below some critical value; i.e., the pore will no longer fill at any pressure below the bulk vapor pressure. Section 5 summarizes our results.

2. Modeling the Interactions

We assume that the sorbate atoms are Lennard-Jonesium with nominal well-depth and size parameters equal to those for argon. Thus, $\epsilon_{gg}/k = 120$ K and $\sigma_{gg} = 3.40$ Å. (In fact, this well-depth will be varied in the simulations over a range from 120 to 240 K in order to explore a range of sorption phenomena.) Modeling of the interactions of these atoms with the pore walls is based on the well-known argon-graphite basal plane energy (Steele, 1978). Thus, each pore wall is taken to be a stack of equally spaced structureless graphite planes with carbon density and plane separation equal to those for graphite. The total energy of an argon atom with this stack of planes is a sum of Lennard-Jones energies over the C sites in the wall, but the sum over the sites in a plane is replaced by an integral. For an infinite plane, this yields a 10-4 function of separation distance with well-depth and size parameters estimated from the experimental data for argon adsorbed on graphite (Steele, 1978). These are $\epsilon_{gs}/k = 58$ K and $\sigma_{gs} = 3.38$ Å. However, the stacks of planes that make up the walls of a square pore are obviously not infinite in extent—they must be truncated to avoid double counting where they meet at the corners of the pore. For simplicity, only one stack is truncated at each corner. An analytic expression for the integrated energy of an atom with a truncated plane has been given elsewhere (Bojan and Steele, 1991). An accurate summation over the planes in an (infinite) stack has been performed numerically. The total argon-pore interaction is then given by the summation of the interactions of an argon in the pore with each of the four walls.

The dimensions of the square cross section of this model pore were carefully chosen so that a 4×4 array of argon sites could be selected that had an argon-argon distance corresponding to the maximum attractive interaction (i.e., at a separation of 3.81 Å) and an argon-wall distance corresponding to the maximum argon-pore wall attractive energy. Contour lines of constant argon-pore interaction $u_s(x, y)$ are shown in Fig. 1, and the locations of the argon lattice points in this cross section are indicated by the filled circles. The separation of sites along the pore axis (z-direction) was also taken to be 3.81 Å.

Figure 1 indicates that the site energies (in units of ϵ_{gs}) are -35 (corner site); -21 (face site); and $= -4.1$ (interior site). These values were used as the basis for an evaluation of the pore filling sequences with variable argon-argon and argon-C site well-depth, as will be described momentarily.

The argon-argon and argon-pore wall interactions described here were also utilized in a straightforward grand canonical Monte Carlo computer simulation of the thermodynamic properties of the pore fluid. The algorithm is well-known (Nicholson and Parsonage, 1969; Allen and Tildesley, 1987) and yields accurate isotherms, energies of adsorption, and local densities of particles and energy. No lattice need be assumed and the simulation can be carried out for any convenient finite temperature. Here, a value of 90 K was selected and the well-depths of the two interaction potentials were varied in an attempt to obtain results that can be compared with the lattice-gas calculations.

3. Lattice-Gas Results

We now evaluate the filling sequence for the simple cubic lattice gas in this pore at $T = 0$. As the configurational part of the chemical potential μ is varied, the pore fills in a way that minimizes the grand potential Ω:

$$\Omega = E(N) - \mu N \tag{1}$$

where $E(N)$ is the energy of the argon in the N filled sites.

The interaction energies are varied by introducing a scaled potential for the various sites. We define a

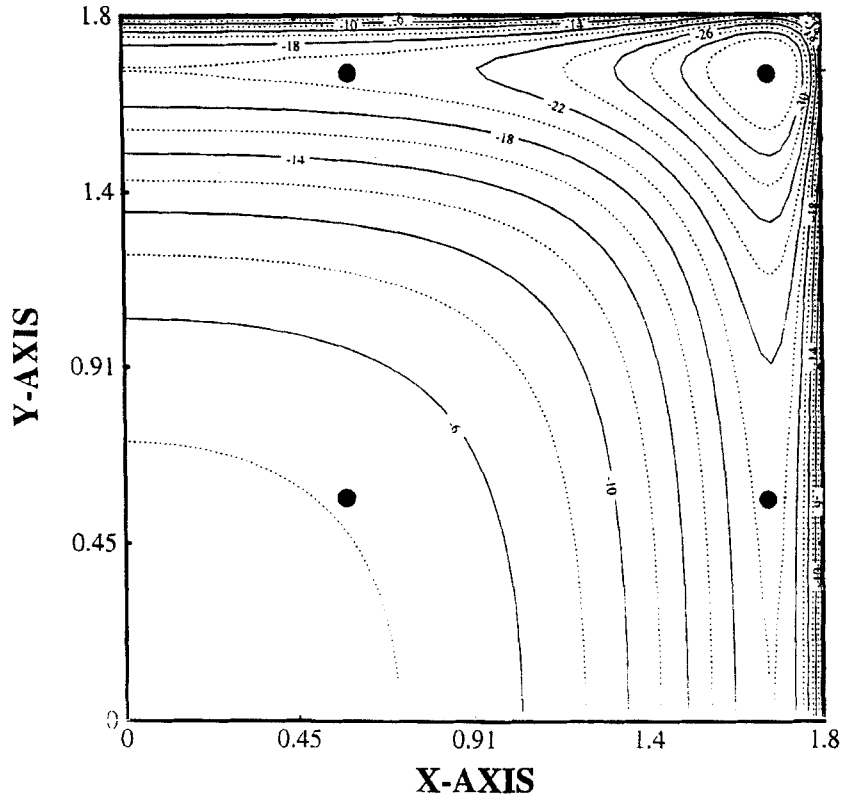

Figure 1. Contour diagram depicting lines of constant energy for the interaction of an Ar atom with the graphite-like walls of a square pore. The x and y dimensions are reduced by 3.40 Å and the energies shown on the contour lines are reduced by ϵ_{gs}. Lattice gas sites are indicated by the black circles.

coupling constant $c = 2\epsilon_{gs}/\epsilon_{gg}$.

$$V_j/\epsilon_{gg} = ce_j \tag{2}$$

where the e_j are constants equal to -17, -10 and -2 for the corner, face and interior sites respectively. The coupling constant has been defined such that $c = 1$ for the sites of the "real" Ar/graphite system (see Fig. 1). We have studied the effects of decreasing c upon the behavior of the pore fluid, and will show how non-wetting occurs at sufficiently small values of this parameter.

If we calculate Ω^* for a single transverse layer of pore sites, we can list values for the following configurations: (Here, all quantities with an asterisk are given in reduced units obtained by dividing by ϵ_{gg}.)

(a) An empty lattice:

$$\Omega^* = 0 \tag{3}$$

(b) All corner sites filled but no other sites occupied (each corner atom has a neighbor in each of the adjacent layers):

$$\Omega^* = -4(17c + 1 + \mu^*) \tag{4}$$

(c) All the corner and face sites are occupied but no site in the interior of the pore (12 atoms per array):

$$\Omega^* = -4(37c + 6 + 3\mu^*) \tag{5}$$

(d) All 16 sites are occupied:

$$\Omega^* = -4(39c + 10 + 4\mu^*) \tag{6}$$

These equations were solved graphically by equating various alternative pairs for Ω^* and thus minimizing this quantity for each given μ^*. The resulting set of lines denote the boundaries of the regions of stability of the configurations listed above. In practice, some of the lines are irrelevant because they involve metastable configurations. Figure 2 presents the resulting transition lines obtained at $T = 0$ for variable c. It can be seen that the pore filling sequence depends sensitively upon this coupling constant. If

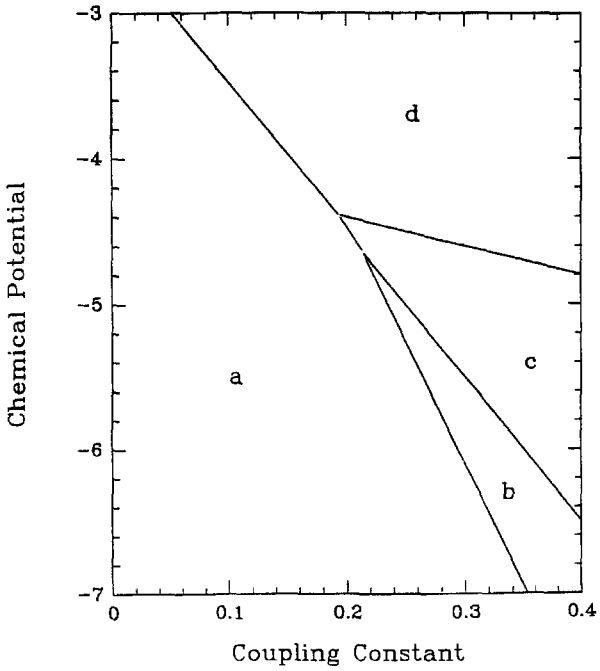

Figure 2. The adsorbed phases at zero temperature are shown as a function of the chemical potential (in units of ϵ_{gg}) and the coupling constant $c = 2\epsilon_{gs}/\epsilon_{gg}$. The labels in the figure refer to the following configurations: (a) empty pore, (b) corner sites occupied, (c) corner and face sites occupied, (d) filled pore.

$c \geq 3/14 \simeq 0.214$, all of the states enumerated above appear as μ^* is varied from $-\infty$ to saturation (-3). If c lies in the narrow interval $0.1935 < c < 3/14$, the state with only filled corner sites does not occur. For $2/39 < c < 0.1935$, the pore filling jumps from empty to full (when $\mu^* = -39c/4 - 5/2$). Finally, if $c < 2/39$, no sorption occurs at all. It is easily shown that this case corresponds precisely to the regime where the full pore energy per particle exceeds that of a particle in the lattice gas bulk phase.

Because this square pore is quasi-one dimensional, the sharp transitions appearing in the $T = 0$ diagram are not present at finite T. In both the lattice gas and the continuum versions of this problem, there do appear rapid variations in coverage with increasing chemical potential which at low T are difficult to distinguish experimentally from a thermodynamic transition.

4. Monte Carlo Calculations

In a grand canonical Monte Carlo simulation, one fixes the value of μ/kT and generates configurations of the atoms in a given (pore) volume by randomly moving atoms to new positions or by creating (destroying) them. Although the length of the computer box used here is 46 Å, periodic boundary conditions along the pore axis are employed to minimize end effects upon the thermodynamic properties of the pore fluid (Swift et al., 1993}). The acceptance probability of any move is governed by an expression that depends upon μ/kT and the potential energy of the system. Thus, the input parameters are ϵ_{gg}/kT, ϵ_{gs}/kT and μ/kT and the output is N_p, the average number of particles in the pore, and the average potential energy of the pore fluid. In contrast to the calculations of Section 3, the simulation produces complete adsorption isotherms in the form μ/kT ($=$ const $+ \ln p$) versus N_p for a given ϵ_{gg}/kT and ϵ_{gs}/kT. Here, the average potential energy will be subdivided into u_{gs} and u_{gg}, the average gas-solid and gas-gas energies, respectively. Other auxiliary quantities of possible interest are the distributions dN/du_{gs} and dN/du_{gg}, the number of fluid atoms dN with gas-solid (or gas-gas) energy between u_{gs} (u_{gg}) and $u_{gs} + du_{gs}$ (u_{gg} and $u_{gg} + du_{gg}$), or $\rho(\mathbf{r})$, the local density of sorbate atoms at point $\mathbf{r}$ within the pore.

For the Lennard-Jones sorbate in this square graphitic pore, two sets of results were simulated: a series of systems with ϵ_{gs}/k fixed at 58 K ("real" graphite) but ϵ_{gg}/k varied from 120 K ("real argon") to 240 K; and a second series with ϵ_{gg}/k fixed at 120 K but ϵ_{gs}/kT varied from 58 K down to 14.5 K. In the second set, it turned out to be convenient to evaluate $\Delta\mu/kT$, where $\Delta\mu = \mu - \mu_{bulk}$, as a function of N_p. (Here, bulk denotes real liquid Ar at 90 K, as represented by a fluid with pairwise additive Lennard-Jones interactions.)

The first set of isotherms generated is shown in Fig. 3 and the second set in Fig. 4. It is clear that steeply rising portions of the isotherms are present in all systems considered, and the dependence of these transitions upon the potential energy parameters is qualitatively similar to that predicted in Section 3. The presence of these steep risers prompted a search for hysteresis between the adsorption and desorption branches. Simulations of the desorption branches were carried out for the systems of Fig. 4 by performing GCMC simulations that started from a computer-generated atomic configuration for a full or nearly full pore. The chemical potential was decreased slightly from that for the stored configuration and the simulation run in the usual way. The GCMC algorithm ensured that the pore loading would decrease during the simulation until (possibly meta-stable) equilibrium was achieved. This procedure was repeated until the chemical potential had decreased

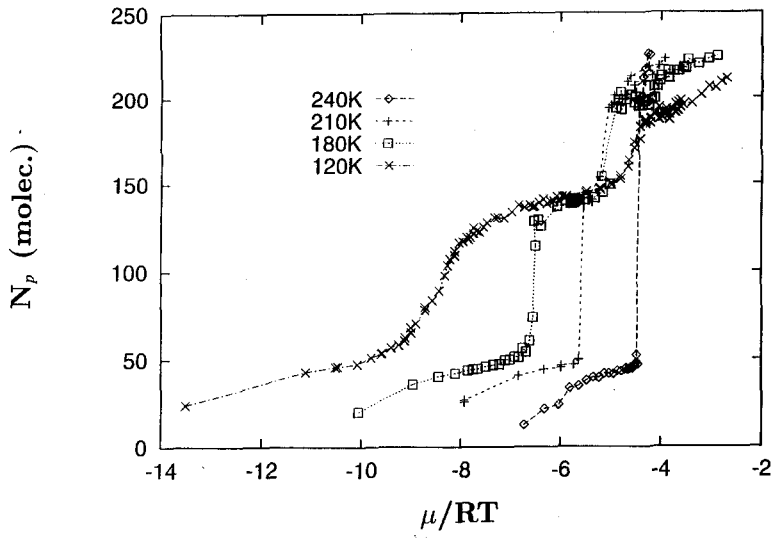

Figure 3. The number of argon atoms in the square pore at 90 K is plotted as a function of the chemical potential for different strengths of the Ar-Ar interaction. The values of ϵ_{gg}/k are indicated in the legend and the well-depth for the Ar-solid interaction was held constant at 58 K.

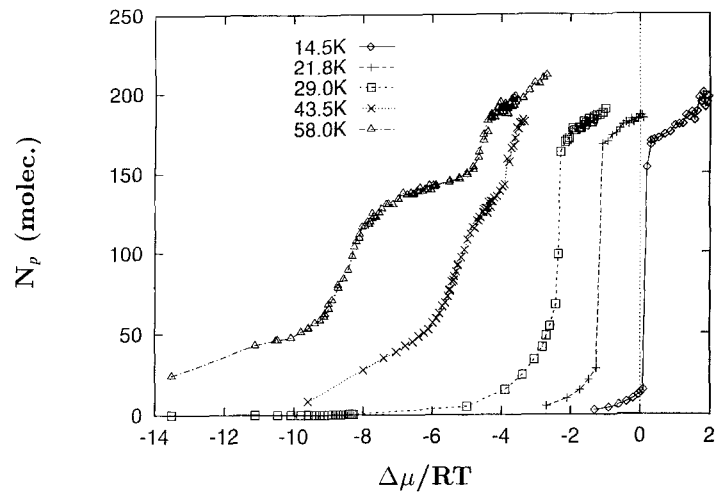

Figure 4. Same as Fig. 3 except the Ar-solid interaction was varied. Here it is the values of ϵ_{gs}/k which are given in the legend while the well-depth for Ar-Ar interaction was held constant at 120 K.

considerably beyond the point corresponding to the steep riser in the adsorption branch. It was observed that adsorption-desorption is completely reversible for the larger values of ϵ_{gs}/k (58.0 and 43.5 K), but a very narrow loop appeared in the isotherm for 29.0 K, and a broader loop for 21.8 K. (The desorption branch was not simulated for the non-wetting case.)

The histograms of u_{gs} for given N_p can help to specify the specific stages of pore filling that correspond to the steeply rising parts of the isotherms of Figs. 3 and 4. For example,histograms of $u^*_{gs} = u_{gs}/\epsilon_{gs}$ are shown for various N_p values in Fig. 5. Distinct peaks appear which correspond to the presence of atoms in the corners with $u_{gs}/\epsilon_{gs} \simeq -35$; atoms on the faces with $u_{gs}/\epsilon_{gs} \simeq= -21$; and interior atoms with $u_{gs}/\epsilon_{gs} \simeq -4$, of course, these peaks have finite widths due to thermal motion in the simulated systems, but otherwise the observed energies are in excellent agreement with those taken in the lattice gas calculations as shown in Fig. 1. An integration under each of these peaks gives the N_p-dependent numbers of atoms sorbed in the corners, on the faces, and in the interiors of each of the

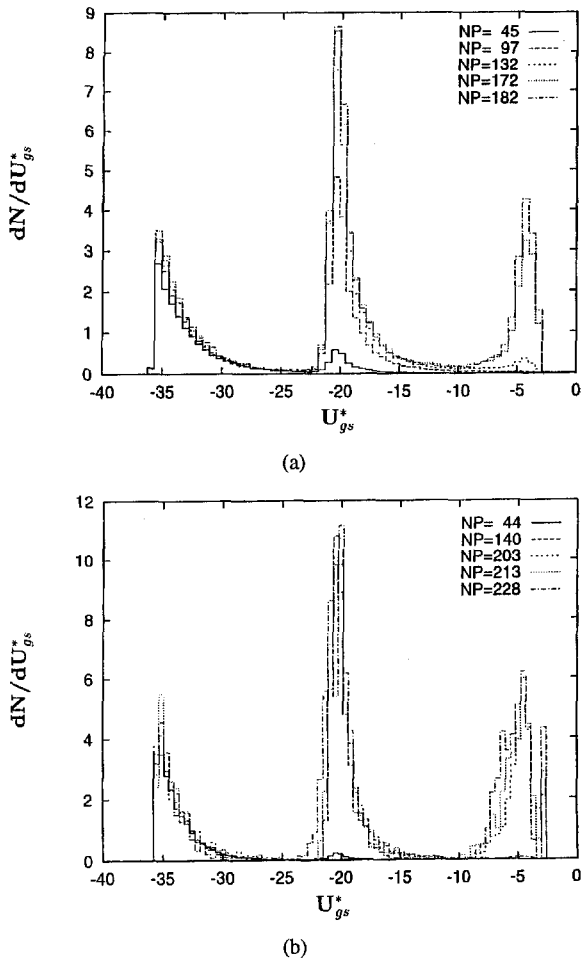

Figure 5. Histograms of the energy distributions of Ar in the square pore at 90 K when (a) $\epsilon_{gg}/k = 120$; $\epsilon_{gs}/k = 43.5$ K and (b) $\epsilon_{gg}/k = 180$ K; $\epsilon_{gs}/k = 58$ K.

pores considered. For the array proposed in Section 2, one would have 12×4 sites in the corners and in the interior, but 12×8 on the faces, giving a total of 192 for a pore of length = 46 Å. The areas under the peaks in the u_{gs} histograms give the numbers of atoms in each region of the pore and thus can be used to construct "local" isotherms. These local isotherms are plots of the numbers of atoms in each region as a function of the total chemical potential. (Alternatively, one can use local densities such as those shown in Figs. 6 and 7 for the same purpose.) Isotherms of this kind are shown in Fig. 8, where it can be seen that sorption in the corners occurs first (at very negative chemical potential). The "corner" isotherms level off at N_a only slightly larger than the number of lattice sites in this region (48). Adsorption on the walls gives isotherms that are shifted to higher μ compared to those for the corners, and the

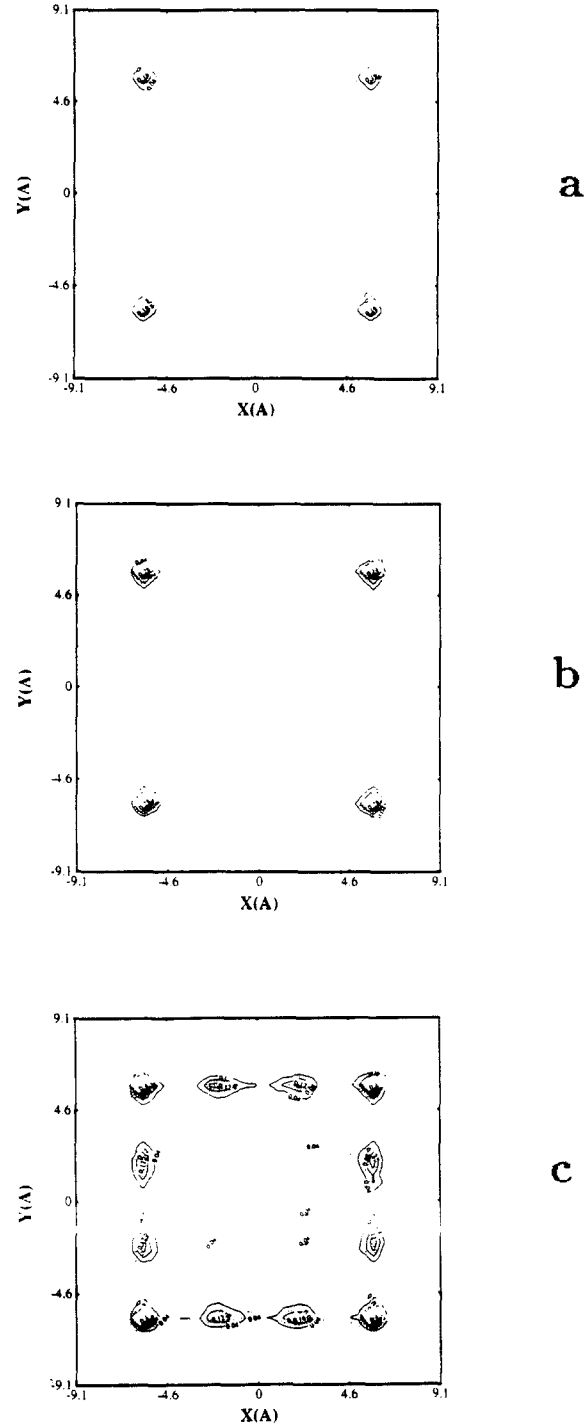

Figure 6. Local densities in the pore evaluated for $\epsilon_{gs}/k = 29$ K ($\epsilon_{gg}/k = 120$ K): (a) $N_p = 24$ (b) $N_p = 54$ (c) $N_p = 169$. The densities are shown for a view down the pore axis. As the number of atoms in the pore increases, the densities indicate that adsorption is primarily sequential (corners first, then walls and finally, interior). Although localization seems to be almost complete in the corners and on the walls, it is clearly much less in the interior volume of the pore—in this respect, the sorbate exhibits at least partial liquid character.

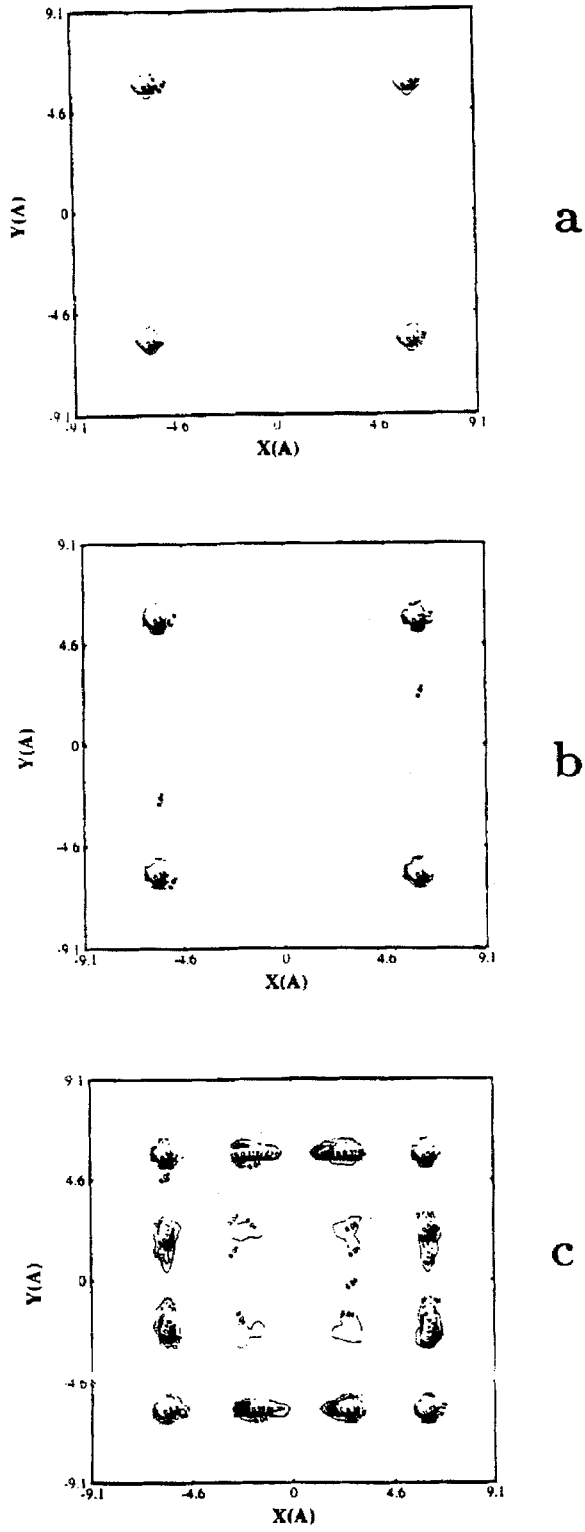

Figure 7. Same as Fig. 6 but for $\epsilon_{gs}/k = 58$ K: (a) $N_p = 24$ (b) $N_p = 57$ (c) $N_p = 185$.

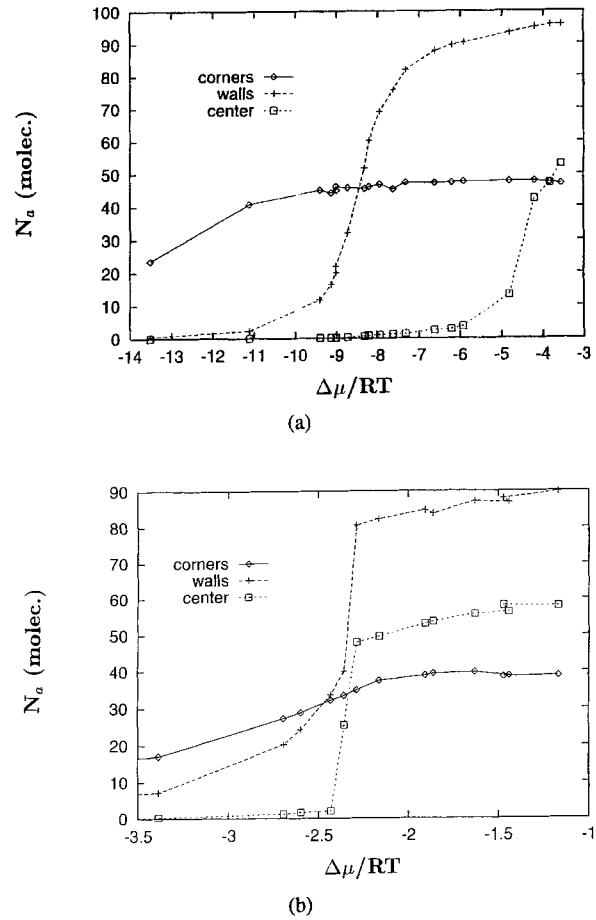

Figure 8. Partial adsorption isotherms are shown here for sorption in specific regions of the pore. Part (a) shows curves calculated from the simulation data for $\epsilon_{gs}/k = 58$ K and $\epsilon_{gg}/k = 120$ K, and part (b) shows these curves for $\epsilon_{gs}/k = 29$ K and $\epsilon_{gg}/k = 120$ K.

limiting amounts adsorbedon the walls is larger than the lattice gas value of 96 atoms. Finally, the sorption in the interior pore volume that occurs last indicates that considerably more atoms are held in this region than the number of such lattice sites (48). It is likely that the sorbate in this volume can be more nearly close-packed than the simple cubic assumed for the lattice gas and, from the local densities shown in Figs. 6 and 7, that it is less likely to be on the points of any lattice.

5. Discussion

In this paper, we have considered two approaches to the problem of capillary condensation in a simple model pore. One is the oversimplified lattice gas model which provides analytic expressions at $T = 0$ and which, as

shown elsewhere (Swift et al., 1993) yields surprisingly accurate results in the mean field limit at finite T. One obvious limitation of this approach is its inability to describe alternative condensed phases (especially liquid, in the present case); this can be important when looking at subtle energy differences of competing structures. Nevertheless, one would hope that the qualitative predictions of capillary filling would be borne out by a more accurate model. We have shown that this is the case by presenting Monte Carlo calculations based on a continuum picture which is designed to be as similar as possible (energetically) to the lattice gas model. In both cases, a sequence of site-filling transitions is found. The larger phase space present in the continuum model at finite T leads to a rounding of the transitions as well as different packing, especially in the interior volume of the pore.

The isotherms in Figs. 3 and 4 can be used to compare the Monte Carlo simulations with the lattice gas phase diagram shown in Fig. 2. For example, the lattice gas model predicts that the coverage jumps from corner to full when $c(= 2\epsilon_{gs}/\epsilon_{gg})$ lies in the interval 0.06 to 0.19. At 90 K, only one of the systems studies shows this behavior: that with $\epsilon_{gg}/k = 120$ K (or $c = 0.5$) in Fig. 3. A similar discrepancy exists between the lattice gas prediction that no atoms will be sorbed at 0 K if $\epsilon_{gs}/\epsilon_{gg} < 0.06$, whereas the simulated isotherms in Fig. 3 indicate that wetting no longer occurs when $\epsilon_{gs} \simeq 14K$ with $\epsilon_{gg} = 120$ K, giving $c \simeq 0.24$. The differences in these c values are not unexpected, considering the large temperature difference involved and the limitations of the lattice model.

It is concluded that the lattice gas model provides a reasonably good guide to the sorption in these model square pores even at 90 K; the sharp transitions at 0 K are made more gradual at finite temperature, as expected, but both calculations indicate that the sorption tends to occur sequentially in the various regions of the pore. Finally, both calculations show that these model pores can become non-wetting for ranges of the energy parameters which are approximately delineated here.

To the extent that they can be separated from the adsorption on the walls and in the interior volume, the portions of the isotherms corresponding to adsorption in the corners of these pores correspond to truly one-dimensional systems (excluding vibrations perpendicular to the chain direction). As expected, there are no signs of steep risers for these parts of the isotherms. Rapid variations in coverage with increasing chemical potential are observed in the simulated isotherms which are difficult to distinguish experimentally from a thermodynamic transition. In all cases, these risers occur in the wall- and interior volume-filling adsorption regions. Since we have here studied pores of only one size, it is not possible to elucidate the dependence of these transitions upon system size. The adsorption-desorption hysteresis observed in the simulated isotherms for the systems of Fig. 4 with the weaker gas-solid interactions is not totally unexpected in view of similar experimental and simulation results for many other porous systems. However, the reason for the dependence of these loops upon the gas-solid interaction strength is not known at present.

Acknowledgment

Support for this research was provided by grant DMR 9022681 of the N.S.F. Division of Material Research.

References

Allen, M.P. and D.J. Tildesley, *Computer Simulation of Liquids*, Oxford University Press, Oxford, 1987.

Bojan, M.J. and W.A. Steele, *Langmuir*, **5**, 625 (1991).

Gregg, S.J. and K.S.W. Sing, *Adsorption, Surface Area and Porosity*, Second Edition Academic Press, London, 1982.

Nicholson, D. and N.G. Parsonage, *Computer Simulation and the Statistical Mechanics of Adsorption*, Academic Press, London, 1982, Norman, G.E. and V.S. Filinov, *High Temperature (Teplofizika Visokikh Temperatur)*, (translated from the Russian) **7**, 216 (1969).

Steele, W.A., *J. Phys. Chem.*, **82**, 817 (1978).

It is known that the difference between the periodic and bulk systems is small if the periodicity length exceeds the pore width. See Swift, M.R., E. Cheng, J.R. Banavar, and M.W. Cole, *Phys. Rev.*, **B48**, 3124 (1993).

The finite temperature version of the calculations of Section 2 is feasible by transfer matrix methods but only if the number of sites in the transverse section is sufficiently small ($\leq$10). See reference (Swift et al., 1993).